JOURNAL OF VIROLOGY, July 1991, p. 3797–3803
0022-538X/91/073797-07$02.00/0

Vol. 65, No. 7

gp160, the Envelope Glycoprotein of Human Immunodeficiency Virus Type 1, Is a Dimer of 125-Kilodalton Subunits Stabilized through Interactions between Their gp41 Domains

D. J. THOMAS,[1,2] J. S. WALL,[3] J. F. HAINFELD,[3] M. KACZOREK,[4] F. P. BOOY,[1] B. L. TRUS,[1,5] F. A. EISERLING,[6] AND A. C. STEVEN[1]*

Laboratory of Structural Biology Research, National Institute of Arthritis and Musculoskeletal and Skin Diseases, Building 6, Room 114,[1] and Division of Computer Research and Technology,[5] National Institutes of Health, Bethesda, Maryland 20892; Laboratoire de Biologie Cellulaire URA-CNRS 256, Université de Rennes I, 35042 Rennes Cedex,[2] and Research and Development, Pasteur Merieux, 27101 Val de Reuil Cedex,[4] France; Department of Biology, Brookhaven National Laboratory, Upton, New York 11973[3]; and Department of Molecular Biology, University of California, Los Angeles, Los Angeles, California 90024[6]

Received 21 December 1990/Accepted 9 April 1991

The molecular masses, carbohydrate contents, oligomeric status, and overall molecular structure of the *env* glycoproteins of human immunodeficiency virus type 1—gp120, gp160, and gp41—have been determined by quantitative electron microscopy. Using purified gp160s, a water-soluble form of *env* purified from a recombinant vaccinia virus expression system, we have measured the masses of several hundred individual molecules by dark-field scanning transmission electron microscopy. When combined with sequence-based information, these mass measurements establish that gp160s is a dimer of subunits with an average monomer mass of 123 kDa, of which ~32 kDa is carbohydrate and 91 kDa is protein. Similarly, gp120 was found to be a monomer of 89 kDa and to contain virtually all of *env*'s glycosylation. gp41 is glycosylated only slightly, if at all, and is responsible for the interactions that stabilize the gp160s dimer. A molecular mass map of gp160s derived by image processing depicts an asymmetric dumbbell whose two domains have masses of ~173 and ~73 kDa, corresponding to a gp120 dimer and a gp41 dimer, respectively. We infer that the average monomer mass of native gp160 is 125 kDa and that in situ, *env* is either a dimer or a tetramer but is most unlikely to be a trimer.

The envelope (*env*) glycoprotein of human immunodeficiency virus type 1 (HIV-1) plays a central role in the transmission and in the pathogenicity of AIDS (2). This protein is initially synthesized as a precursor with a nominal mass of 160 kDa (gp160), which is subsequently cleaved to its gp120 and gp41 moieties (1, 8, 25, 31). gp41 contains the cytoplasmic and transmembrane portion(s) of gp160, whereas gp120 constitutes its external domain(s) (3). In infected cells, interactions between gp41 and other viral constituents are implicated in the budding event of the final phase of viral assembly. Specific sites on gp120 bind to the CD4 receptor protein which is present on the surface of helper T lymphocytes, macrophages, and other susceptible cells (6), thus determining the tissue selectivity for viral infection. This binding facilitates the uptake of the virus particle by fusion of its envelope with the host cell membrane, another function mediated by the *env* glycoproteins (34). Neutralizing antibodies against HIV have been found to be directed against epitopes on both gp120 and gp41 (7, 18, 24).

In view of its involvement in these important viral functions, knowledge of the structure of the HIV envelope glycoprotein is central to an understanding of viral pathogenesis and infectivity at the molecular level. Although its primary sequence is now known for many strains of HIV (27, 40), knowledge of *env*'s molecular structure remains scanty. The monomer molecular weights of gp160 and gp120 are nominal values assigned on the basis of their electrophoretic mobilities in denaturing gels and, in both cases, greatly exceed the values predicted from their cDNA sequences. Moreover, these molecules are known to be heavily—and perhaps variably—glycosylated (17, 26), and a protein's electrophoretic mobility may be substantially changed by the covalent attachment of carbohydrates. Similarly, the oligomeric status of HIV-1 *env* has been in doubt, monomers (30), dimers (9), trimers (10, 15, 43), and tetramers (9, 29, 32) having been advocated by different investigators.

The goal of this study has been to use quantitative scanning transmission electron microscopy (STEM) (42) to effect an unambiguous determination of the molecular weights of gp160 and gp120. The physical basis of this method is the elastic scattering of electrons by the component atoms of the scanned molecules. Unstained molecules yield a dark-field signal that is proportional to their local mass density. Accordingly, after subtraction of the background contributed by the carbon support film, integration of the image density associated with a given particle yields its mass, when calibrated against a reference specimen of known molecular weight. When sequence-derived information on the monomer's molecular weight is taken into account, STEM measurements of molecules' masses allow their oligomeric character to be determined. Similarly, the carbohydrate contents of glycoproteins may be deduced. Image processing of the STEM micrographs allows the spatial distribution of mass within the particle to be described (35, 42). From such two-dimensional mass maps, the masses of specific features may be calculated. Here, we report the application of these techniques to purified gp160s and gp120. The STEM mass map is also compared with the

* Corresponding author.

corresponding image derived by conventional negative-staining electron microscopy.

MATERIALS AND METHODS

Production and purification of *env* glycoproteins. gp160s is a derivative of the *env* glycoprotein of the LAV/BRU strain of HIV-1 (40), from which both its cleavage site and the most hydrophobic segment (Phe-690 to Val-710) in the gp41 segment of the molecule have been deleted (20). gp160s secreted from BHK-21 cells infected with a recombinant vaccinia virus was purified by gel filtration and lentil lectin affinity chromatography (20), followed by reverse-phase high-pressure liquid chromatography (7a). Purity was higher than 90% as assessed from the chromatography elution profile.

STEM. STEM was performed at the Brookhaven Resource (41). In a typical experiment, an aliquot from the original sample (4.3 mg of protein per ml in phosphate-buffered saline) was diluted 250× into 10 mM ammonium acetate (pH 7.5) and then dialyzed for 2 h against the same buffer. A 5-μl sample was then injected into a drop of buffer previously applied to a carbon film mounted on a microscope grid and allowed to absorb for 1 min. Tobacco mosaic virus (TMV) was added, and the grid was washed three times with 10 mM ammonium acetate (pH 7.5) and then freeze-dried at a constant sublimation rate over a period of 6 to 8 h. During observation, the specimens were maintained at −150°C on a liquid N_2-cooled stage. Images were recorded directly in digital form.

Conventional transmission electron microscopy. For negative staining, proteins were diluted to 20 μg/ml and then dialyzed against 10 mM ammonium acetate (pH 7.5) for 2 h. Typically, a drop was then applied to a thin carbon film mounted on a fenestrated thick carbon film on a microscope grid, washed three times with 10 mM ammonium acetate (pH 7.5), and stained with a 1% solution of uranyl acetate. Images were recorded on a Zeiss EM902 electron microscope at a nominal magnification of ×30,000 under low-dose conditions.

Computer image processing. From the STEM data, the masses of many individual particles were determined by integration of the cumulative density in appropriate subareas of the micrographs (35, 41). Conventional transmission electron micrographs of areas showing a suitable coverage of molecules in a continuous stain layer were checked for microscopic quality by optical diffraction and then digitized by using a Perkin-Elmer 1010MG microdensitometer, at a scan rate corresponding to 0.6 nm at the specimen. These images were analyzed on a VAX 8350 computer running the PIC software system (38). Particles adjudged by visual criteria to be of morphotype A (approximately 30% of all particles) were aligned by correlation methods (35, 37). After alignment and before averaging, the data set was screened to eliminate statistically anomalous particles (found to be 15 to 20% of the total) by means of the OMO algorithm (39). The averaged STEM image was produced in essentially the same way except that with these data, compensation was also made for the sparse sampling of the specimen by the finely focused STEM probe (35).

Experimental uncertainty. (i) Random errors. The random errors implicit in STEM mass determinations have been analyzed in depth (41, 42). The margin of error decreases as the specimen mass increases, and it is expected to be in the range of ±13% (standard deviation) for molecules in the 100-kDa mass range and ±7% for 250-kDa particles, under the conditions (film thickness, electron dose, and area integrated) applicable to our measurements. In practice, the dispersions of sets of multiple measurements tend to be larger than this treatment predicts. For this reason, in Table 1 we have reported standard deviations, as well as standard errors of the mean, as indicators of experimental uncertainty.

(ii) Systematic errors. Of the potential sources of systematic error, the most likely are incomplete washing of the specimen (residual salts would increase its apparent mass) and mass loss through radiation damage (decreasing its apparent mass). The presence of residual salt manifests itself in STEM micrographs as a visibly nonuniform background in the vicinity of the specimen. No such contamination was observed around the *env* protein molecules whose analysis is reported.

With regard to mass loss, all proteins lose mass at the same rate when irradiated by 40-keV electrons (41). Since TMV (which is 95% protein) was used for calibration, and it loses mass at the same rate as the specimen, radiation-induced mass loss should result in an increased random error, not a systematic error, where proteins are concerned. In any case, under the conditions used in our experiments, viz., −150°C specimen temperature and electron doses of 2 to 5 electrons per 0.01 nm^2, mass loss from protein is very small, 1 to 2% at most (42).

Concerning glycoproteins, current evidence suggests that their carbohydrate moieties may be somewhat, but not drastically, more susceptible to mass loss than their polypeptide moieties (40a). Taking a fivefold difference in volatility as a reasonable upper limit, we may calculate what the resulting bias in STEM mass measurements of glycoproteins would be. With electron doses that cause 1.5% mass loss from polypeptides and with TMV for calibration, the STEM-derived mass would be low by 1.5% for a glycoprotein that is 25% carbohydrate by mass and by 3% for one that is 50% carbohydrate.

RESULTS

STEM of unstained *env* glycoproteins. Our experiments used a recombinant form of gp160 (gp160s) expressed in mammalian cells. gp160s was rendered water soluble by the deletion of a highly hydrophobic sequence of 21 residues from gp41 and was rendered resistant to gp120 conversion by modification of the cleavage site (20). A typical dark-field STEM image of the purified protein is shown in Fig. 1. The particles' dimensions are fairly uniform, of the order of 15 to 20 nm, but they exhibit considerable morphological variation. We have operationally defined five classes (morphotypes), of which representative galleries are shown in Fig. 2. The most frequently occurring class, morphotype A, accounting for 25 to 30% of all particles, has a bilobed, somewhat elongated appearance (Fig. 2A). Three other morphotypes are B (elongated, but not evidently bipartite), C (trilobed), and D (relatively compact and globular) (Fig. 2B to D). The fifth class is more diverse and consists of those particles that do not conform to the criteria that define the four specific morphotypes.

Individual particle masses were determined for several hundred gp160s molecules by two-dimensional integration of the image densities. The global distribution is shown in Fig. 3a. The overwhelming majority of particles (>90%) comprise a homogeneous population that averages 246 kDa (Table 1). In addition, there is a minority component at about 120 to 135 kDa (e.g., Fig. 2A, +), and a few particles have higher molecular masses. When the mass distributions of

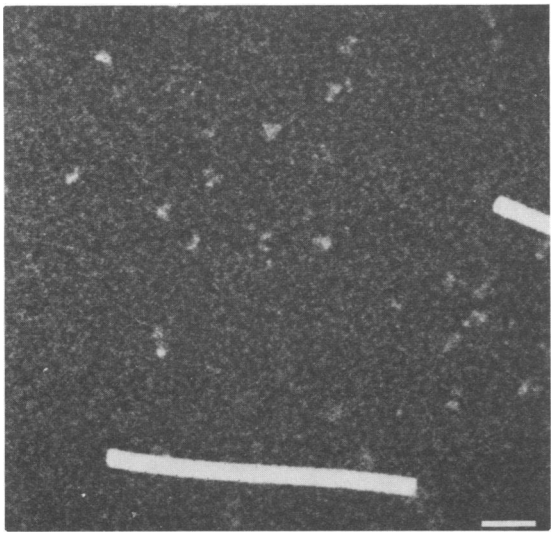

FIG. 1. Dark-field STEM micrograph of gp160s molecules, visualized unstained after freeze-drying. The dense rods are TMV particles, used as an internal mass standard (42). Bar = 50 nm.

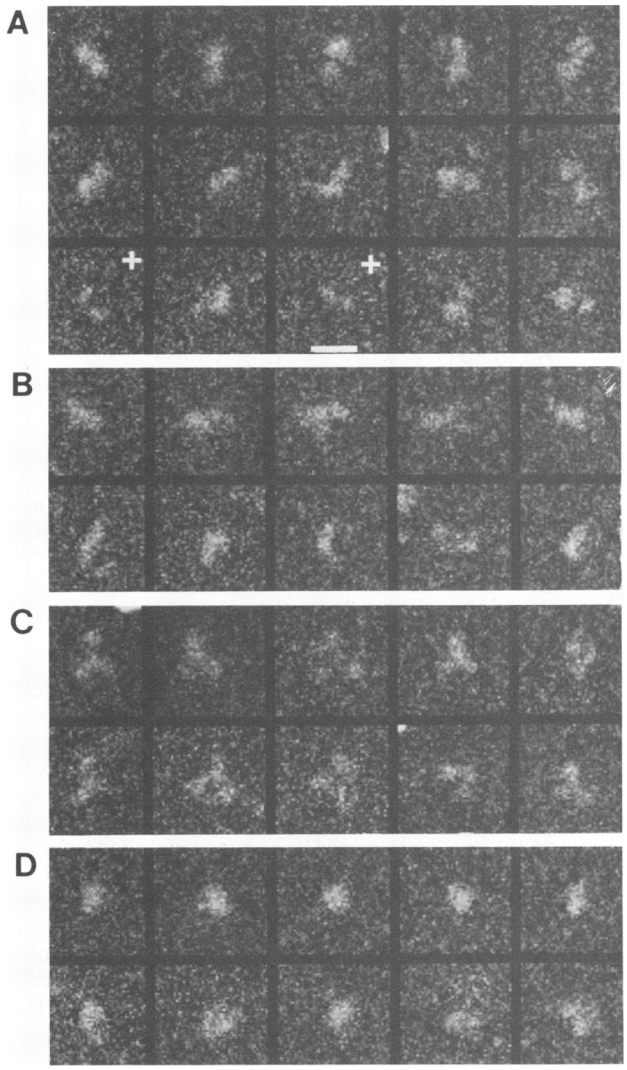

FIG. 2. Galleries of various morphological classes of particles visualized in dark-field STEM micrographs of unstained, freeze-dried preparations of gp160s. Panels A to D show representatives of morphotypes A to D, respectively. The masses of these particles are all in the vicinity of 250 kDa, except for the particles marked with a plus sign in panel A, which are about 125 kDa. Bar = 20 nm.

morphotypes A to D are considered separately, they are found to be indistinguishable, all averaging ~250 kDa. Thus we conclude that the various morphotypes do not represent different oligomeric states of gp160s, as might have been hypothesized a priori on the grounds of the monolobed, bilobed, and trilobed appearances of morphotypes D, A, and C, respectively; rather, they represent different views or, possibly, different conformations or states of preservation of the same molecule. The few particles with higher molecular masses almost all belong to the morphologically heterogeneous class E and presumably represent either higher-order aggregates or contaminants.

Similar analyses were performed with purified gp120 produced in the same recombinant vaccinia virus expression system (20). In our STEM images, these particles were globular in appearance and 8 to 10 nm in diameter and showed no evident indications of substructure (data not shown). The resulting distribution of particle masses is unimodal, averaging 89 kDa (Fig. 3b; Table 1).

For comparison, we also performed STEM mass measurements on a preparation of gp120 purchased from MicroGenesys Inc., West Haven, Conn. (gp120M), which had been expressed in a recombinant baculovirus system. The resulting data yielded a multicomponent distribution, corresponding to subunits of 90 kDa and multiples thereof. Since both forms of gp120 studied had the same monomer mass, we conclude that the two proteins had undergone similar patterns of glycosylation, despite their different origins (gp120 was expressed in mammalian cells, and gp120M was expressed in insect cells). That the gp120M which we analyzed were not homogeneously in a single oligomeric state may reflect differences between the respective purification procedures, expression systems, or molecular designs.

Molecular structure of gp160s. Closer examination of morphotype A particles (Fig. 2a) indicates that their two lobes are generally unequal. This aspect becomes clearer in the noise-suppressed representation obtained by correlation averaging (Fig. 4a). From this mass map, the partitioning of the total molecular mass between the two domains may be determined: they contain ~173 and ~73 kDa, respectively. The large domain is oblate in shape, with a width of 12 nm and a height of 9 nm. The smaller domain is approximately spherical and 8 nm in diameter.

In negative stain, the gp160s molecules are also quite heterogeneous in appearance (data not shown), but subpopulations corresponding to the major morphotypes detected in the STEM data may be readily identified. Correlation averaging was also performed on these data. The resulting image of morphotype A particles largely confirms the morphology revealed in the STEM image derived from unstained, freeze-dried molecules (cf. Fig. 4a and b). The length of the molecule is quite consistent in these two images, but the major lobe is somewhat narrower in the negatively stained representation.

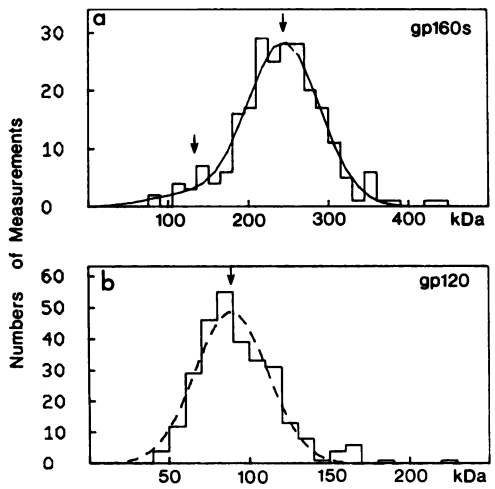

FIG. 3. Histograms of particles mass measurements determined for gp160s (a) and gp120 (b). The curve in panel b represents the sum of two Gaussian components, whose means are marked (arrows).

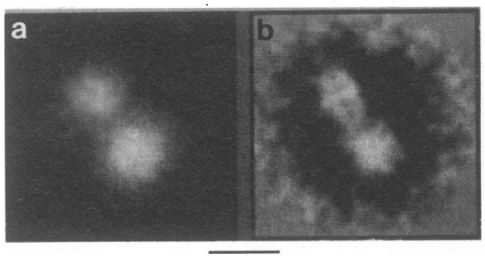

FIG. 4. Computer-averaged representations of gp160s as unstained, freeze-dried in STEM (a) and after negative staining and visualized by conventional bright-field transmission electron microscopy (b). There is good overall agreement between the respective representations of the molecule. The distinction in size between the major and minor domains is somewhat less pronounced in negative stain, which probably reflects less efficient stain exclusion by the carbohydrate moieties. Bar = 20 nm.

DISCUSSION

Molecular masses of gp160 and gp120. STEM possesses unique advantages for the direct determination of molecular masses of macromolecules in situations in which polydispersity, asymmetric or elongated shape, or paucity of experimental material may compromise or invalidate other experimental procedures (12, 41). The procedure has been validated by results obtained for numerous oligomeric and polymeric proteins (reviewed in references 12 and 42). Perhaps the best-characterized test specimen to date is the glutamine synthetase dodecamer from *Escherichia coli*, whose mass was determined as 626 ± 27 (standard deviation) kDa by STEM (23) and whose sequence-derived molecular mass was subsequently determined to be 12 × 51.782 kDa = 621.384 kDa (5, 44). There have been fewer analyses as yet of proteins that are substantially glycosylated. However, since the electron scattering characteristics of polysaccharides are very similar to those of protein, the method should be equally applicable to glycoproteins (11). The best-documented application so far is clotting factor V (20 to 25% carbohydrate) (28), for which the STEM results are in good agreement with earlier hydrodynamic data and with sequence-derived information on the molecular mass.

The STEM determination yields a value of 123 kDa for the average monomer mass of gp160s and a value of 89 kDa for gp120. The monomer mass of native gp160 should be slightly greater than that of gp160s, by the amount corresponding to the deletion, i.e., an additional 2.1 kDa of polypeptide, giving a total mass of 125 kDa. There are no potential glycosylation sites in the deleted segment to which additional carbohydrates could be attached. These molecular masses are considerably lower than the nominal values that were assigned on the basis of electrophoretic mobility. A systematic trend of sodium dodecyl sulfate (SDS)-polyacrylamide gel electrophoresis to underestimate the molecular weights of heavily glycosylated proteins has previously been noted (4, 21, 33). This effect has been attributed to the failure of carbohydrate to bind SDS stoichiometrically with the protein (33).

TABLE 1. Mass species present in preparations of purified *env* glycoproteins of HIV-1 as determined by STEM analysis[a]

Molecule	Molecular mass (kDa)			Fraction (% of measurements)
	Average	SD	SEM	
gp160s (n = 233)	246	±40	±3	94
	135	±43	±10	6
gp120 (n = 274)	89	±22	±2	100

[a] In each case, the complete set of individual mass measurements was histogrammed (Fig. 3), and the resulting distributions were then described by a Gaussian curve, or a sum of two such curves, whose parameters (mean, standard deviation, and amplitude) were determined by means of a generalized least-squares fit (36).

Oligomeric status of gp160s and gp120. Calculated from their respective amino acid sequences, the polypeptide chains corresponding to gp160s and gp120 have molecular masses of 91 and 54 kDa, respectively. The molecular mass of gp160s, at 246 kDa, would be insufficient for a trimer, even in the absence of any glycosylation. We conclude that it is a dimer of 123-kDa subunits, each of which contains ~32 kDa of carbohydrates, in addition to 91 kDa of protein. Unlike the only other possibility—that gp160s is a monomer—interpretation of the 246-kDa particle as a dimer unifies all of our observations in a straightforward and self-consistent way. In particular, the minority of particles at 120 to 140 kDa (e.g., Fig. 2A, +) represent dissociated subunits but cannot be accounted for by the monomer scenario.

env glycoproteins have been the subject of a number of studies using ultracentrifugation (9, 10), gel electrophoresis (29, 30, 43) in conjunction with chemical cross-linking (32), and conventional electron microscopy (15), leading to conflicting conclusions with respect to molecular stoichiometry. Qualitatively our findings are in agreement with the conclusions of Earl et al. (9), who studied broad *env*-containing peaks on sucrose gradients loaded with detergent extracts from infected cells. Quantitatively, however, we note that their deduction of a dimer from the sedimentation coefficient (10.8S) is predicated on the assumption of a monomer molecular mass of 160 kDa for gp160. If this calculation is repeated using instead the value of 125 kDa determined in this study, it corresponds to a stoichiometry of 2.5 subunits, consistent with either a dimer or a trimer.

Implications for native gp160. Although our data show quite clearly that gp160s is a dimer, they do not rule out the possibility that gp160 forms a tetramer, i.e., a double dimer, in situ (32). Either the deletion of the hydrophobic segment

from gp41 in gp160s or the purification procedure may have affected the protein's tendency to oligomerize further. However, whereas there are documented cases of mutants of oligomeric proteins that fail to oligomerize (e.g., reference 16), we are not aware of any mutants that form a well-defined oligomer with the incorrect number of subunits. (We distinguish here between partial oligomerization, i.e., an assembly intermediate, and formation of an oligomer of a different order, with no evident role as a discreet subassembly. Polymerization into higher-order structures, for which there are many examples of polymorphism resulting from misassembly, is a different matter!) On this basis, we consider it very unlikely that gp160 is a trimer in situ.

Mutant strains of HIV-1 in which cleavage of gp160 is suppressed remain competent for viral assembly, but the resulting particles are noninfectious, being deficient in fusogenicity and having a diminished affinity for the CD4 receptor (19, 20). It may be that cleavage of gp160 induces a conformational change that is required for these functions. However, any such change does not appear to affect the gross morphology of the glycoprotein, since the oblate shape and dimensions of the major domain of our gp160s dimer (Fig. 4a) match quite well those of HIV-1 spikes visualized in thin sections of virus particles (14) (and which presumably represent gp120 since cleavage precedes delivery of the protein to the cell surface). HIV-1 spikes are distinctly oblate (14), in contrast to the radially extended spikes of many other viral envelopes. However, the uncertainty implicit in dimensional measurements from such images does not allow one to use them to settle the question of whether the spike is a dimer or a tetramer in situ.

Carbohydrate contents of gp160, gp120, and gp41. gp120 purified from our expression system (20) consists exclusively of monomers made up of 54 kDa of protein and 35 kDa of carbohydrates, essentially the same amount that is present on gp160s itself. Subtraction of the measured mass of gp120 from that of gp160s gives a monomer mass of 34 kDa for gp41, in good agreement with the value calculated from its sequence (~37 kDa). The margin of error in the mass measurements (Table 1; see Materials and Methods) does not rule out the possibility that gp41 may be slightly glycosylated, and it has recently been reported that exposure of gp41 to deglycosylation treatment results in a slightly altered electrophoretic mobility (13). However, our data indicate that virtually the entire carbohydrate content of gp160s, some 32 to 35 kDa, is located on its gp120 moiety.

In a recent report, Leonard et al. (22) listed 24 potential sites on gp120 and presented evidence that all are occupied, at least on some molecules, although they also noted that their data were indicative of heterogeneous glycosylation. Moreover, gp160 and gp120 both run as very diffuse bands on SDS-gels, which is strongly suggestive of chemical heterogeneity. Most likely, this is due to variable glycosylation, which inevitably means less than complete glycosylation. Our estimate of 34 kDa of carbohydrate per molecule suggests that, at 2 kDa per chain, on average, about 17 of 24 (71%) are occupied, and somewhat fewer when complex carbohydrates are taken into account. Bearing in mind that the recombinant gp120 of Leonard et al. (22) was produced in CHO cells and ours was produced in BHK cells (and could therefore have undergone somewhat different glycosylation patterns), there is no evident contradiction between the two lines of evidence.

Domainal divisions and intersubunit interactions in gp160. Our mass data are consistent with the interpretation of the major domain of gp160s (~173 kDa) as a dimer of gp120 and its minor domain (~73 kDa) as a dimer of gp41. The dimeric nature of gp160s is further suggested by the presence in the averaged negatively stained image of a faint striation that bisects the molecule along its long axis (Fig. 4b). Moreover, the monomeric state of isolated gp120 indicates that in the gp160s dimer, the gp120 subunits are less stably associated than are the gp41 subunits. Thus, our data strongly suggest that the interactions between gp41 subunits are primarily responsible for stabilizing the gp160 dimer, and they corroborate earlier evidence to this effect (9, 29).

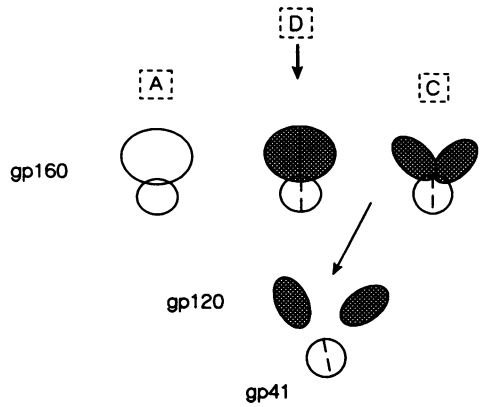

FIG. 5. Diagram indicating how the various morphological classes of particle detected by electron microscopy of purified gp160 and gp120 may be produced as different views, or decomposition products of a dimeric gp160 molecule. In D, the arrow indicates that the molecule is viewed from above, from which direction it projects a globular shape. A, D, and C correspond to the morphotypes observed, as illustrated in Fig. 2.

Moreover, this property provides a plausible explanation for gp160s particles of morphotype C as molecules in which the two gp120 domains have separated but remain linked by their gp41 domains, resulting in three domains of approximately equal size (Fig. 2C). How the gp160 dimer may give rise to the various morphological entities observed is shown schematically in Fig. 5. Morphotype D most likely represents particles viewed approximately parallel to their long axis, and morphotype B most likely represents particles in which the division between the major and minor domains is not well visualized.

The major lobe of gp160s, which we have interpreted as a dimer of gp120, appears narrower in negative stain (Fig. 4). Possibly, this may signify less efficient exclusion of stain by their carbohydrate moieties, which would imply that the glycosylation is concentrated primarily around the sides of these molecules and not at their distal ends or the intersubunit interface.

In conclusion, the mass map and the consistent negatively stained projection defined here for the gp160s dimer (Fig. 4a) provide a molecular projection which should serve as a frame of reference for further, more detailed structural studies based on electron microscopy and digital image processing. In particular, comparative studies of gp160s complexed with soluble CD4 or antibodies of defined specificity should allow determination of the relative positions of functionally important sites and antigens in the overall complex.

ACKNOWLEDGMENTS

We are grateful to I. Diaz and M. Ollivier (Pasteur Merieux) for preparation and purification of proteins, to M. Simon (BNL) for STEM operation, to B. Lin (BNL) for specimen preparation, and to M. Bisher (LSBR-NIAMS) for photography.

This work was supported in part (J.S.W. and J.F.H.) by the OHER of the U.S. Department of Energy and by NIH grants RR01777 (to J.S.W.) and AI25319 (to F.A.E.).

REFERENCES

1. **Allan, J. S., J. E. Coligan, F. Barin, M. F. McLane, J. D. Sodroski, C. A. Rosen, W. A. Haseltine, T. H. Lee, and M. Essex.** 1985. Major glycoprotein antigens that induce antibodies in AIDS patients are encoded by HTLV-III. Science **228**:1091–1094.
2. **Barré-Sinoussi, F., J. C. Chermann, F. Rey, M. T. Nugeyre, S. Chamaret, J. Gruest, C. Dauguet, C. Axler-Blin, F. Vezinet-Brun, C. Rouzioux, W. Rozenbaum, and L. Montagnier.** 1983. Isolation of a T-lymphotropic retrovirus from a patient at risk for acquired immune deficiency syndrome (AIDS). Science **220**:868–871.
3. **Berman, P. W., L. Riddle, G. Nakamura, O. K. Haffar, W. M. Nunes, P. Skehel, R. Byrn, J. Groopman, T. Matthews, and T. Gregory.** 1989. Expression and immunogenicity of the extracellular domain of the human immunodeficiency virus type 1 envelope glycoprotein, gp160. J. Virol. **63**:3489–3498.
4. **Bretscher, M. S.** 1971. Major human erythrocyte glycoprotein spans the cell membrane. Nature (London) New Biol. **231**:229–232.
5. **Colombo, G., and J. J. Villafranca.** 1986. Amino acid sequence of *Escherichia coli* glutamine synthetase deduced from the DNA nucleotide sequence. J. Biol. Chem. **261**:10587–10591.
6. **Dalgleish, A. G., P. C. Beverley, P. R. Clapham, D. H. Crawford, M. F. Greaves, and R. A. Weiss.** 1984. The CD4 (T4) antigen is an essential component of the receptor for the AIDS retrovirus. Nature (London) **312**:763–767.
7. **Dalgleish, A. G., T. C. Chanh, R. C. Kennedy, P. Kanda, P. R. Clapham, and R. A. Weiss.** 1988. Neutralization of diverse HIV-1 strains by monoclonal antibodies raised against a gp41 synthetic peptide. Virology **165**:209–215.

7a. **Diaz, I., and M. Ollivier.** Unpublished data.

8. **DiMarzo Veronese, F., A. L. DeVico, T. D. Copeland, S. Oroszlan, R. C. Gallo, and M. G. Sarngadharan.** 1985. Characterization of gp41 as the transmembrane protein coded by the HTLV-III-LAV envelope gene. Science **229**:1402–1404.
9. **Earl, P. L., R. W. Doms, and B. Moss.** 1990. Oligomeric structure of the human immunodeficiency virus type 1 envelope glycoprotein. Proc. Natl. Acad. Sci. USA **87**:648–652.
10. **Einfeld, D., and E. Hunter.** 1988. Oligomeric structure of a prototype retrovirus glycoprotein. Proc. Natl. Acad. Sci. USA **85**:8688–8692.
11. **Engel, A.** 1983. Mass determination by electron scattering. Micron **13**:425–436.
12. **Engel, A.** 1980. Current state of biological scanning transmission electron microscopy, p. 170–178. *In* W. Baumeister and W. Vogell (ed.), Electron microscopy at molecular dimensions. Springer-Verlag, Berlin.
13. **Fenouillet, E., J. C. Gluckman, and E. Bahraoui.** 1990. Role of N-linked glycans of envelope glycoproteins in infectivity of human immunodeficiency virus type 1. J. Virol. **64**:2841–2848.
14. **Gelderblom, H. R., E. H. S. Hausmann, M. Ozel, G. Pauli, and M. A. Koch.** 1987. Fine structure of human immunodeficiency virus (HIV) and immunolocalization of structural proteins. Virology **156**:171–176.
15. **Gelderblom, H. R., M. Ozel, and G. Pauli.** 1989. Morphogenesis and morphology of HIV: structure-function relationships. Arch. Virol. **106**:1–13.
16. **Gething, M.-J., K. McCammon, and J. Sambrook.** 1986. Expression of wild-type and mutant forms of influenza hemagglutinin: the role of folding in intracellular transport. Cell **46**:939–950.
17. **Geyer, H., C. Holschbach, G. Hunsmann, and J. Schneider.** 1988. Carbohydrates of human immunodeficiency virus: structure of oligosaccharides linked to the envelope glycoprotein gp120. J. Biol. Chem. **263**:11760–11767.
18. **Goudsmit, J., C. Debouck, R. H. Meloen, L. Smit, M. Bakker, D. M. Asher, A. V. Wolff, C. J. Gibbs, Jr., and D. C. Gajdusek.** 1988. Human immunodeficiency virus type 1 neutralization epitope with conserved architecture elicits early type-specific antibodies in experimentally infected chimpanzees. Proc. Natl. Acad. Sci. USA **85**:4478–4482.
19. **Guo, H.-G., F. diMarzo Veronese, E. Tschachler, R. Pal, V. S. Kalyanraman, R. C. Gallo, and M. S. Reitz, Jr.** 1990. Characterization of an HIV-1 point mutant blocked in envelope glycoprotein cleavage. Virology **174**:217–224.
20. **Kieny, M. P., R. Lathe, Y. Riviere, K. Dott, D. Schmitt, M. Girard, L. Montagnier, and J.-P. Lecocq.** 1988. Improved antigenicity of the HIV env protein by cleavage site removal. Protein Eng. **2**:219–225.
21. **Leach, B. S., J. F. Collawn, and W. W. Fish.** 1980. Behavior of glycoproteins with empirical molecular weight estimation methods. 1. In sodium dodecyl sulfate. Biochemistry **19**:5734–5741.
22. **Leonard, C. K., M. W. Spellman, L. Riddle, R. J. Harris, J. N. Thomas, and T. J. Gregory.** 1990. Assignment of intrachain disulfide bonds and characterization of potential glycosylation sites of the type 1 recombinant human immunodeficiency virus envelope glycoprotein (gp120) expressed in Chinese hamster ovary cells. J. Biol. Chem. **265**:10373–10382.
23. **Lipka, J. J., J. F. Hainfeld, and J. S. Wall.** 1984. Undecagold labelling of glutamine synthetase from *E. coli*. Proc. 42nd Annu. Meet. EMSA, p. 158–159.
24. **Matsushita, S., M. Robert-Guroff, J. Rusche, A. Koito, T. Hattori, H. Hoshino, K. Javaherian, K. Takatsuki, and S. Putney.** 1988. Characterization of a human immunodeficiency virus neutralizing monoclonal antibody and mapping of the neutralizing epitope. J. Virol. **62**:2107–2114.
25. **McKeating, J. A., and R. L. Willey.** 1989. Structure and function of the HIV envelope. AIDS **3**:S35–S41.
26. **Mizuochi, T., M. W. Spellman, M. Larkin, J. Solomon, L. J. Basa, and T. Feizi.** 1988. Carbohydrate structures of the human immunodeficiency virus (HIV) recombinant envelope glycoprotein gp120 produced in Chinese hamster ovary cells. Biochem. J. **254**:599–603.
27. **Modrow, S., B. H. Hahn, G. M. Shaw, R. C. Gallo, F. Wong-Staal, and H. Wolf.** 1987. Computer-assisted analysis of envelope protein sequences of seven human immunodeficiency virus isolates: prediction of antigenic epitopes in conserved and variable regions. J. Virol. **61**:570–578.
28. **Mosesson, M. W., W. R. Church, J. P. DiOrio, S. Krishnaswamy, K. G. Mann, J. F. Hainfeld, and J. S. Wall.** 1990. Structural model of factors V and Va based on scanning transmission electron microscope images and mass analysis. J. Biol. Chem. **265**:8863–8868.
29. **Pinter, A., W. J. Honnen, S. A. Tilley, C. Bona, H. Zaghouani, M. K. Gorny, and S. Zolla-Pazner.** 1989. Oligomeric structure of gp41, the transmembrane protein of human immunodeficiency virus type 1. J. Virol. **63**:2674–2679.
30. **Rey, M.-A., B. Krust, A. G. Laurent, L. Montagnier, and A. G. Hovanessian.** 1989. Characterization of human immunodeficiency virus type 2 envelope glycoproteins: dimerization of the glycoprotein precursor during processing. J. Virol. **63**:647–658.
31. **Robey, W. G., B. Safai, S. Oroszlan, L. O. Arthur, M. A. Gonda, R. C. Gallo, and P. J. Fischinger.** 1985. Characterization of envelope and core structural gene products of HTLV-III with sera from AIDS patients. Science **228**:593–595.
32. **Schawaller, M., G. E. Smith, J. J. Skehel, and D. C. Wiley.** 1989. Studies with cross-linking reagents on the oligomeric structure of the *env* glycoprotein of HIV. Virology **172**:367–369.
33. **Segrest, J. P., and R. L. Jackson.** 1972. Molecular weight determination of glycoproteins by polyacrylamide gel electrophoresis in the presence of sodium dodecyl sulfate. Methods Enzymol. **28**:54–63.
34. **Stein, B. S., S. D. Gowda, J. D. Lifson, R. C. Penhallow, K. G. Bensch, and E. G. Engleman.** 1987. pH-independent HIV entry into CD4-positive T-cells via virus envelope fusion to the plasma membrane. Cell **49**:659–668.
35. **Steven, A. C., B. L. Trus, J. V. Maizel, M. Unser, D. A. D.**

Parry, J. S. Wall, J. F. Hainfeld, and F. W. Studier. 1988. The molecular substructure of a viral receptor-recognition protein—the gp17 tail-fiber of bacteriophage T7. J. Mol. Biol. **200**:351–365.

36. **Steven, A. C., J. S. Wall, J. F. Hainfeld, and P. M. Steinert.** 1982. The structure of fibroblastic intermediate filaments: analysis by scanning transmission electron microscopy. Proc. Natl. Acad. Sci. USA **79**:3101–3105.
37. **Thomas, D., M. J. Flifla, B. Escoffier, M. Barray, and E. Delain.** 1988. Image processing of electron micrographs of human alpha2-macroglobulin half-molecules induced by Cd^{+}. Biol. Cell. **64**:39–44.
38. **Trus, B. L., and A. C. Steven.** 1981. Digital image processing of electron micrographs—the PIC system. Ultramicroscopy **6**:383–386.
39. **Unser, M., A. C. Steven, and B. L. Trus.** 1986. Odd men out: a quantitative objective procedure for identifying anomalous members of a set of noisy images of ostensibly identical specimens. Ultramicroscopy **19**:337–348.
40. **Wain-Hobson, S., P. Sonigo, O. Danos, S. Cole, and M. Alizon.** 1985. Nucleotide sequence of the AIDS virus, LAV. Cell **40**:9–17.

40a. **Wall, J.** Unpublished data.

41. **Wall, J.** 1979. Biological scanning transmission electron microscopy, p. 333–342. *In* J. J. Hren, J. I. Goldstein, and D. C. Joy (ed.), Introduction to analytical electron microscopy. Plenum Publishing Corp., New York.
42. **Wall, J. S., and J. F. Hainfeld.** 1986. Mass-mapping with the scanning transmission electron microscope. Annu. Rev. Biophys. Biophys. Chem. **15**:355–376.
43. **Weiss, C. D., J. A. Levy, and J. M. White.** 1990. Oligomeric organization of gp120 on infectious human immunodeficiency virus type 1 particles. J. Virol. **64**:5674–5677.
44. **Yamashita, M. M., R. J. Almassy, C. A. Janson, D. Cascio, and D. Eisenberg.** 1989. Refined atomic model of glutamine synthetase at 3.5Å resolution. J. Biol. Chem. **264**:17681–17690.